the basic respiratory rhythm is a small class of preBötC rhythmogenic neurons (type 1) onto which several modulatory systems converge. These neurons may overlap or even be identical to other preBötC neurons with intrinsic oscillatory bursting properties—for example, pacemaker neurons (*3, 19*) and preinspiratory neurons (*20*)—because 50% of type 1 neurons have bursting properties (*16*) and at least some project to the midline (*21*). However, whether endogenous burst activity is critical for generation of respiratory rhythm per se (*3, 18–20*) remains to be determined. Alterations in peptidergic transmission in the preBötC may play a role in respiratory disorders such as sleep apnea (*22*) and sudden infant death syndrome (*23*). The possibility that multiple peptide systems affecting respiration converge on a particular identifiable class of neurons represents an interesting locus for ventilatory control. The coexpression within the ventrolateral respiratory column of NK1R and μOR in preBötC neurons provides an opportunity to exploit targeted molecular manipulation of breathing in animal models and a basis for analysis of human respiratory disorders.

References and Notes

1. A. L. Bianchi, M. Denavit-Saubie, J. Champagnat, *Physiol. Rev.* **75**, 1 (1995); J. L. Feldman, in *Handbooks of Physiology: The Nervous System. Intrinsic Regulatory System in the Brain*, F. Bloom, Ed. (American Physiological Society, Bethesda, MD, 1986), pp. 463–524; E. G. Dobbins and J. L. Feldman, *J. Comp. Neurol.* **347**, 64 (1994).
2. J. C. Rekling and J. L. Feldman, *Annu. Rev. Physiol.* **60**, 385 (1998).
3. J. C. Smith, H. H. Ellenberger, K. Ballanyi, D. W. Richter, J. L. Feldman, *Science* **254**, 726 (1991).
4. A. Monnier, F. Hayashi, D. R. McCrimmon, *Soc. Neurosci. Abstr.* **346**, 5 (1998); N. Koshiya and P. G. Guyenet, *J. Physiol. London* **491**, 859 (1996); J. M. Ramirez, S. W. Schwarzacher, O. Pierrefiche, B. M. Olivera, D. W. Richter, *J. Physiol. London* **507**, 895 (1998); J. H. Hsieh *et al.*, *J. Autom. Nerv. Sys.* **73**, 7 (1998).
5. J. L. Feldman and J. C. Smith, *Ann. NY Acad. Sci.* **563**, 114 (1989).
6. S. M. Johnson, J. C. Smith, J. L. Feldman, *J. Appl. Physiol.* **80**, 2120 (1996).
7. J. Brockhaus and K. Ballanyi, *Eur. J. Neurosci.* **10**, 3823 (1998).
8. A. C. Bonham, *Resp. Physiol.* **101**, 219 (1995); D. R. McCrimmon and G. S. Mitchell, in *Regulation of Breathing*, J. A. Dempsey and A. I. Pack, Eds. (Dekker, New York, 1995), vol. 79, pp. 151–218.
9. G. D. Funk, J. C. Smith, J. L. Feldman, *J. Neurophysiol.* **70**, 1497 (1993); X. M. Shao and J. L. Feldman, *J. Neurophysiol.* **77**, 1853 (1997).
10. H. L. Fields and M. M. Heinricher, *Philos. Trans. R. Soc. London Ser. B* **308**, 361 (1985).
11. Transverse 400- or 800-μm-thick slices of the brainstem from BALB/c mice (P_0–P_3) and Sprague-Dawley rats (P_0–P_4) were cut at the level of the caudal and rostral preBötC, respectively, as reported (*3*) and perfused in artificial cerebrospinal fluid (aCSF) containing 128 mM NaCl, 9 mM KCl, 0.5 mM NaH_2PO_4, 1.5 mM $CaCl_2$, 1.0 mM $MgSO_4$, 23.5 mM $NaHCO_3$, 30 mM glucose (rat), or 130 mM NaCl, 5.4 mM KCl, 0.8 mM KH_2PO_4, 26 mM $NaHCO_3$, 30 mM glucose, 1 mM $MgCl_2$, 0.8 mM $CaCl_2$ (mouse). Rhythmic respiratory-related motor output was recorded by a suction electrode placed on a XII nerve rootlet. Nerve activity was amplified, filtered at 3 Hz to 1 kHz, and rectified nerve activity was integrated. SP, DAMGO, 4,5,6,7-tetrahydroisoxazolo[5,4-c]pyridin3-ol (THIP) hydrochloride, glycine, and TTX were obtained from RBI and dissolved in aCSF. Drugs were microinjected with glass micropipettes (tip diameter 6 to 12 μm) lowered (100 to 300 μm) into the preBötC by micromanipulator. Injections were made with a controlled pressure source for 5 s. Ejection volume was monitored with a calibrated eyepiece reticule.
12. Female adult Sprague-Dawley rats (n = 17) and BALB/c mice (n = 2) were transcardially perfused with 4% paraformaldehyde in phosphate-buffered saline (PBS) with or without picric acid, cryoprotected in 25% sucrose PBS, embedded in OCT, sectioned at 25 to 40 μm on a cryostat, and processed free floating. Sections were incubated in primary antibody diluted in serum at 4°C for 24 to 48 hours, placed in fluorescent (Jackson Immunoresearch) or biotin (Vector Laboratories) conjugated species-specific secondary antibody overnight, and mounted on gelatin-subbed slides. In several rats, μOR immunohistochemistry was amplified with tyramine signal amplification–direct green amplification (NEN Lifesciences) and bright-field NK1R staining was visualized with a Vectastain Elite ABC kit and diaminobenzidine. Antibodies: rabbit antibody to NK1R (anti-NK1R) (1:2500 fluorescent, 1:25,000 bright field; Chemicon), guinea pig anti-$GABA_BR$ (1:3000; Chemicon), goat anti-ChAT (1:100; Chemicon), mouse anti-TH (1:1000; Boehringer Mannheim), rabbit anti-μOR (1:75,000 TSA or 1:7000 fluorescent; Instar). Bright-field images were digitally acquired (Polaroid DMC) into Photoshop (Adobe Systems) and background subtracted to remove chip nonlinearities. Confocal images were acquired with a Zeiss 410 SCM and maximal intensity projections were generated in NIH Image. All images were filtered and adjusted for contrast and light levels in Photoshop for clarity. Cell counts for coexpression were obtained by visual inspection of confocal images (n = 2).
13. P. A. Gray and J. L. Feldman, data not shown.
14. J. L. Feldman and H. H. Ellenberger, *Annu. Rev. Physiol.* **50**, 593 (1988); H. H. Ellenberger, J. L. Feldman, W. Z. Zhan, *J. Comp. Neurol.* **294**, 212 (1990); H. H. Ellenberger and J. L. Feldman, *J. Comp. Neurol.* **294**, 202 (1990).
15. Neurons located at the caudal or rostral part of the preBötC in mice were visualized with differential interference contrast and infrared video microscopy. Glass micropipettes (resistances typically were 2 to 3 MW) were filled with a solution containing 115 mM $HMeSO_3$, 115 mM KOH, 5 mM NaCl, 1 mM $MgCl_2$, 0.01 mM $CaCl_2$, 0.1 mM BAPTA [1,2-bis(2-aminophenoxy)ethane-*N*,*N*,*N*′,*N*′-tetraacetic acid, tetra-K^+ salt], 10 mM Hepes, 3 mM 2-ATP(Mg^{2+}) (pH 7.3). Current- or voltage-clamp recordings were made with an Axoclamp-2A (Axon Instruments) amplifier in bridge or single electrode voltage clamp mode. The *I-V* relationship was determined by injecting a slow (7-s cycle) ramp-shaped current and plotting the rising phase of the *I-V*. Signals were recorded on videocassette (pulse code modulation; Vetter Instruments, model 3000A), digitized at 1 to 20 kHz with a Digidata 1200 A/D board (Axon Instruments) and analyzed with Axoscope software (Axon Instruments). Statistical values are given as mean ± SEM.
16. J. C. Rekling, J. Champagnat, M. Denavit-Saubié, *J. Neurophysiol.* **75**, 811 (1996).
17. ———, *J. Neurophysiol.* **75**, 795 (1996).
18. R. J. Butera Jr., J. Rinzel, J. C. Smith, *J. Neurophysiol.* **82**, 382 (1999); *J. Neurophysiol.* **82**, 398 (1999).
19. N. Koshiya and J. C. Smith, *Nature* **400**, 360 (1999).
20. H. Onimaru, A. Arata, I. Homma, *Jpn. J. Physiol.* **47**, 385 (1997).
21. J. C. Rekling and J. L. Feldman, data not shown.
22. E. Fletcher and J. Schaff, in *Abnormalities of Respiration During Sleep*, E. Fletcher, Ed. (Grune & Stratton, Orlando, FL, 1986), pp. 203–228; E. C. Fletcher, *Cardiologia* **42**, 469 (1997); S. Thalhofer and P. Dorow, *Respiration* **64**, 2 (1997).
23. J. P. Orlowski, *Pediatrics* **78**, 233 (1986); V. Carpentier, H. Vaudry, E. Mallet, A. Laquerrière, P. Leroux, *Neuroscience* **86**, 159 (1998); A. Coquerel *et al.*, *Neurochem. Int.* **20**, 97 (1992).

24. Supported by a Ford Foundation Pre-Doctoral Fellowship for Minorities and a predoctoral fellowship from the Porter Physiology Development Program of the American Physiological Society to P.A.G., a Parker B. Francis Fellowship to J.C.R., and NIH grants HL40959 and HL37941. We thank N. Brecha, D. Buonomono, L. Kruger, and F. Schweizer for assistance with this manuscript.

12 July 1999; accepted 8 October 1999

Identification of a Conserved Receptor-Binding Site on the Fiber Proteins of CAR-Recognizing Adenoviridae

Peter W. Roelvink,* Gai Mi Lee, David A. Einfeld, Imre Kovesdi, Thomas J. Wickham

The human adenovirus serotype 5 (Ad5) is used widely for applications in human gene therapy. Cellular attachment of Ad5 is mediated by binding of the carboxyl-terminal knob of its fiber coat protein to the Coxsackie adenovirus receptor (CAR) protein. However, Ad5 binding to CAR hampers the development of adenovirus vectors capable of specifically targeting (diseased) tissues or organs. Through sequence analysis and mutagenesis, a conserved receptor-binding region was identified on the side of three divergent CAR-binding knobs. The feasibility of simultaneous CAR ablation and redirection of an adenovirus to a new receptor is demonstrated.

The human adenovirus family has 49 viral serotypes that are associated with a wide range of pathologies and tissue tropisms (*1, 2*). The serotype Ad5 has been studied intensively and is currently used as a vector in human gene therapy (*3*). Cellular attachment is mediated by binding of the COOH-terminal knob of the adenovirus fiber coat protein

to the CAR protein by serotypes from five of the six adenovirus subgroups (*1, 4–11*). The fiber knob amino acid sequences among these serotypes vary widely. These serotypes, despite the divergence in the knob sequence of 29 to 66% relative to the fiber 5 knob (F5K), all recognize CAR (*10, 12*), which implies a conservation of the amino acids or motifs involved in receptor binding. We aligned the knob amino acid sequences of 14 adenoviruses from the subgroups that have CAR-binding serotypes, and scored the identity and similarity (*13*). As expected, only very few amino acids, in similar positions, were conserved in the structure (Fig. 1, A and B). Unexpectedly, this analysis identified a conserved cluster of amino acids on the side of the fiber trimer. The crystallographic model for the Ad5 knob predicts that this cluster is mostly surface-exposed (*14, 15*). Very little amino acid conservation was observed for the exposed receptor face (R sheet) on top of the protein, which has been hypothesized to interface with CAR (*14, 15*).

We have mutagenized the majority of the amino acids present in the exposed loops and β sheets on the top and the side of the F5K protein, including the conserved cluster, and expressed all mutants in insect cells (*16*). The majority of mutant proteins were expressed as soluble proteins, as evaluated by protein immunoblot and detection by an affinity-purified polyclonal antibody to the knob (*4*). Trimerization was evaluated by binding with mouse monoclonal antibodies (mAbs) that only recognize the native knob trimer (*17*). All mutants that were found to be soluble and trimeric are shown on the F5K map (Fig. 1, C and D).

The mutant proteins were tested in competition assays for their ability to inhibit the transduction of CAR-expressing A549 cells by an Ad.CMV-βgal vector (*9, 18*). Because transduction first involves binding to CAR, the ability of mutant knob proteins to compete for this receptor, and thus block transduction, can be assessed indirectly. By determining the amount of protein needed to inhibit 50% of transduction for the wild-type F5K protein (IC_{50}) and comparing that to the IC_{50} values obtained for the mutant proteins, the reduction in affinity for CAR can be estimated. Mutation of six critical residues of F5K, all located on the side of the fiber knob protein structure (Fig. 1, B and D), either completely or partially failed to block transduction of A549 cells by Ad.CMV-βgal (Fig. 2, A and B): S408E or G, P409A, K417G or L (AB loop), K420A (B β sheet), Y477A or T (DE loop), and Y491A (FG loop) (*19*). In addition, a four–amino acid deletion of the sequence TAYT (d489-492) or replacement of the sequence EGTAY in the FG loop with glycine residues (r487-491) also completely failed to inhibit Ad.CMV-βgal transduction of the A549 cells. A replacement mutant where the amino acids DPE that precede the critical residue Y477 in the DE loop are replaced with glycines (r474-476) had a partially inhibitory effect. Three point mutations in the AB loop, and one in the proximal B β sheet, overlap with the conserved cluster on the side of the fiber knob (Fig. 1, B and D) and yield mutant proteins with IC_{50} values two to more than three orders of magnitude greater than that for wild-type F5K protein (Fig. 2A). This suggests conservation of critical residues among CAR-binding adenoviruses and demonstrates that the AB loop is a crucial element of the CAR-binding site. Mutational analysis of the FG loop sequence EGTAY showed that only Y491A resulted in an IC_{50} that was two orders of magnitude greater than that of wild-type F5K protein (Fig. 2B).

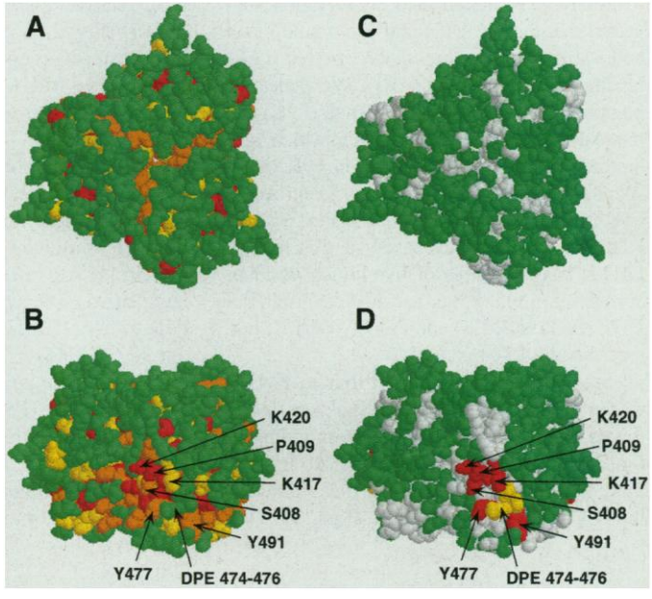

Fig. 1. (**A** and **B**) Variability and conservation analysis of CAR-binding fiber protein sequences. The amino acid sequences of 14 fiber knobs were aligned by the Megalign program, which uses the Jotun-Hein algorithm with a PAM (point accepted mutations per 200 aligned positions) 250-residue weight table. Colors were assigned on the basis of sequence identity score in each of the positions of the alignment (red, 93 to 100%; orange, 71 to 86%; yellow, 57 to 64%; green for any lower score). (**C** and **D**) Mutants in loops and β sheets. Point mutations that reduce the fiber-CAR interaction by two to more than three orders of magnitude, as measured by IC_{50} in a competition assay, are red. The mutation r474-476, which resulted in an IC_{50} value five times that of wild-type F5K, is shown in yellow. Mutations that did not affect CAR binding are green. Residues that were not mutated are gray.

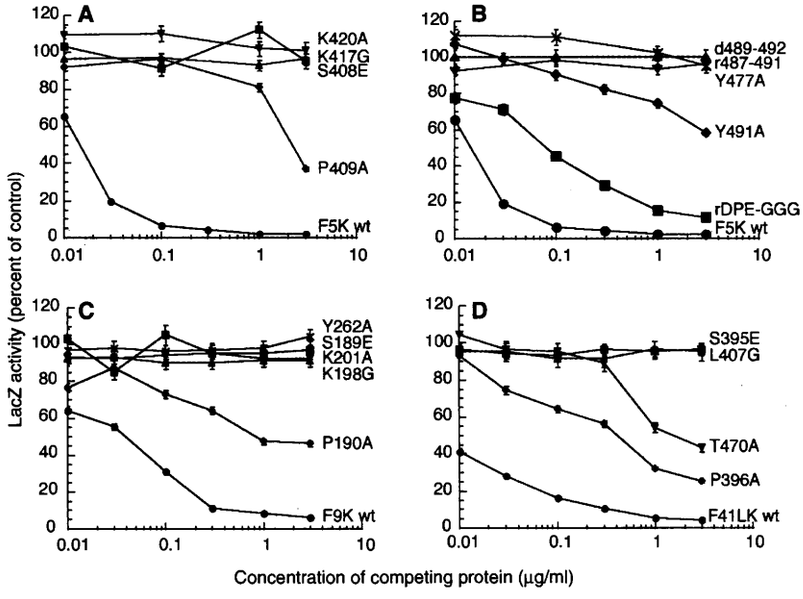

Fig. 2. Competition-expression assay analysis of mutant fiber knob proteins. (**A**) F5K AB loop and B β sheet mutants. (**B**) F5K DE and FG loop mutants. (**C**) F9K mutants. (**D**) F41LK mutants.

Research and Development, GenVec Inc., 65 West Watkins Mill Road, Gaithersburg, MD 20879, USA.

*To whom correspondence should be addressed. E-mail: genecloner@genvec.com

As the Y491 residue is partially buried (Fig. 1B), this mutation possibly alters structural conformation of the CAR-binding site. This implies that the FG loop may play an indirect role in binding the CAR protein. All point mutants having an IC_{50} that was more than two orders of magnitude greater than that of F5K were generally conserved between different serotypes (Fig. 1, B and D). All mutations to the R sheet blocked CAR-mediated transduction as efficiently as wild-type F5K protein, indicating that this structure is not critical to receptor binding (*14, 15, 20*).

Analysis of amino acid conservation suggested that the CAR-binding site would likely be localized in the same region of other CAR-binding fiber knobs (Fig. 1B). We generated point mutants in the Ad9 fiber knob (F9K) and the Ad41L fiber knob (F41LK), which also bind to CAR (*10*). All residues in F9K corresponding to the critical residues identified in F5K (that is, F9K residues S189, P190, K198, K201, and Y262) are conserved. In contrast, F41LK has only three of five critical residues conserved (S395, P396, and K407); instead of F5K residues K417 and Y477, F41LK has, respectively, L404 and T470.

Five residues in F9K and four in F41LK were mutagenized. From our analyses, it followed that all the residues corresponding to those that were found to be critical to CAR binding in F5K also were critical to CAR binding in F9K and F41LK. Thus, the F9K mutations S189E, K198G, K201A, and Y262A (Fig. 2C)—corresponding to F5K residues S408, K417, K420, and Y477—all have IC_{50} values that are at least three orders of magnitude greater than that of their native wild-type protein. The same is true for the F41LK mutations S395E and L407G (Fig. 2D), corresponding to F5K residues S408 and K417, respectively. The F9K mutation P190A and the F41LK mutations P396A and T470A (corresponding to F5K residues P409, K420, and Y477, respectively) resulted in mutants with a 25- to 100-fold increase in IC_{50} relative to that of wild-type F9K or F41LK (Fig. 2, C and D). Thus, all the residues corresponding to those that were found to be critical to CAR binding in the F5 knob also were critical to CAR binding in the F9 and F41L knobs.

To test the hypothesis that the amino acids identified as critical are truly part of a putative CAR-binding site, we analyzed the binding of F5K mutant proteins to soluble CAR protein [sCAR (*10*)] and to the non-neutralizing mAb 3D9, which recognizes only the F5K trimer (*17*). The mutations that knocked out sCAR binding, as well as the mutations that defined the epitopes of mAb 3D9, were mapped on the F5K protein (Fig. 3). The sCAR protein failed to bind to, or had reduced affinity for, the trimeric F5K mutants that failed to compete in competition assays (lane 1). Three mutations—K506R, the partial FG loop replacement rSHGKTA-GSGSGS 507-512 (r507-512), and the HI loop deletion/replacement rGTQETGDT-TPSA-GSGG 538-549 (dr538-549)—did not abrogate sCAR binding. These mutations did abrogate mAb 3D9 binding (Fig. 3, lane 2), indicating that the FG and HI loops are part of its epitope. These mutant proteins, however, were recognized by mAbs 2C9 and 3F10, which also only recognize the native F5K trimer (*17*).

We next sought to demonstrate that the mutations we have identified can be used to construct an adenovirus vector that lacks native CAR binding and is also redirected to a novel receptor. We introduced the CAR ablating mutation d489-492 TAYT into the vector Adf, which expresses green fluorescent protein (GFP) as a marker. In addition, the tag YPYDVPDYA, which corresponds to the epitope recognized by a mAb raised against the hemagglutination (HA) protein of influenza virus (*21*), was inserted into the HI loop of the fiber. The resultant vector Adf.F(TAYT-HA) was generated using standard techniques (*22*) and has a particle/plaque-forming unit ratio comparable to that of Ad5 vectors (*23*). We evaluated the transduction by this new vector of the cell lines 293 (which expresses CAR) and 293-HA (which expresses both CAR and a novel receptor, a membrane-tethered single-chain antibody to the HA epitope) (*23*). When we added equal numbers of particles of Adf.F(TAYT-HA) or Adf to 293 cells, we observed that transduction of the cells by Adf.F(TAYT-HA) was reduced by two orders of magnitude relative to Adf (Fig. 4, A and B). In contrast, transduction of 293-HA cells by Adf.F(TAYT-HA) was equal to transduction by Adf (Fig. 4, C and D). Transduction was quantified by counting the number of transduced cells in a microscopic field (~1000 cells per field, eight fields counted). The vector Adf transduced 293 cells at 117 ± 12 cells per field, whereas Adf.F(TAYT-HA) transduced only 0.7 ± 0.3 cells. For 293-HA cells, transduction by Adf and by Adf.F(TAYT-HA) was comparable (105 ± 26 and 114 ± 22 cells per field, respectively). This low-level residual transduction can be blocked by penton base protein, but not by recombinant fiber protein (*20*). This finding suggests that the penton base mediates the majority of this residual transduction.

We conclude that the CAR-binding site consists of residues from the AB loop, the B β sheet, and the DE loop—that is, F5K resi-

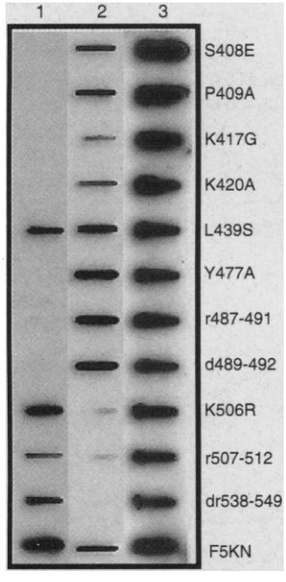

Fig. 3. Binding of soluble CAR and 3D9 mAb to mutant knob proteins. Proteins (5 μg) were blotted on nitrocellulose and incubated for 2 hours in phosphate-buffered saline, pH 7.4, with 5% milk powder. The blots were incubated overnight with sCAR protein (2 μg/ml, lane 1), mAb 3D9 (lane 2), or a 1:5000 dilution of a rabbit polyclonal antibody to the F5K protein, as a control (lane 3) (*4*). Further procedures were as described (*10*).

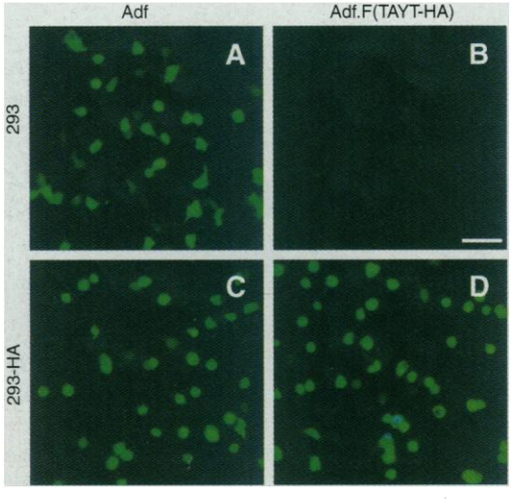

Fig. 4. Transduction of 293 and 293-HA cell lines by Adf (**A** and **C**) and the CAR ablated vector Adf.F(TAYT-HA) (**B** and **D**). Cells at a density of 10^6 cells per 35-mm well were infected with the adenovirus vector at 10 physical particles per cell and incubated for 1 hour at 37°C. Cells were briefly washed with DMEM + 5% FCS and incubated overnight in the same medium. GFP was visualized on a Nikon fluorescent microscope equipped with the appropriate filters. Scale bar, 50 μm.

dues S408, P409, K417, K420, and Y477. This site is located on the side of the knob, maps to a single monomer, and does not overlap two adjacent monomers. This finding implies that the trimeric knob binds to three CAR molecules independently, and it agrees with a determination of the molecular mass of the Ad12 fiber knob complexed with the IgV domain of the CAR protein (*24*).

The fiber knobs of the CAR-binding serotypes display profound dissimilarity of the loops (distal DE, distal FG and HI) that surround the critical residues, which indicates a potential role for these structures in avoiding neutralizing immunity. An analogous situation may exist for the human immunodeficiency virus gp120 envelope glycoprotein (*25–27*) and the sialic acid binding site of the hemagglutinin protein of influenza viruses (*28, 29*).

Our experiments with the vector Adf.F-(TAYT-HA) demonstrate the feasibility of combined CAR-binding ablation and simultaneous retargeting to a new receptor by introduction of new targeting sequences to an adenovirus vector fiber protein. Incorporation of this concept into adenoviral gene therapy vectors will lead to the development of safer, targeted vectors capable of delivering therapeutic genes to tissues with the highest possible specificity.

Note added in proof: Bewley *et al.* (*30*) have analyzed the crystal structure of the CAR-recognizing Ad12 fiber knob complexed with the D1 domain of the CAR protein. Their study confirms that the fiber AB loop plays an essential role in the interaction with the cellular receptor protein, CAR.

References and Notes

1. T. Shenk, in *Fields Virology*, B. N. Fields, D. M. Knipe, P. M. Howley, Eds. (Lippincott-Raven, Philadelphia, 1996), vol. 2, pp. 2111–2148.
2. D. Schnurr and M. E. Dondero, *Intervirology* **36**, 79 (1993).
3. M. Horwitz, in *Virology*, B. N. Fields and D. M. Knipe, Eds. (Raven, New York, 1990), vol. 2, pp. 1679–1721.
4. L. J. Henry, D. Xia, M. E. Wilke, J. Deisenhofer, R. D. Gerard, *J. Virol.* **68**, 5239 (1994).
5. N. Louis, P. Fender, A. Barge, P. Kitts, J. Chroboczek, *J. Virol.* **68**, 4104 (1994).
6. P. W. Roelvink, I. Kovesdi, T. J. Wickham, *J. Virol.* **70**, 7614 (1996).
7. S. C. Stevenson, M. Rollence, B. White, L. Weaver, A. McClelland, *J. Virol.* **69**, 2850 (1995).
8. R. P. Tomko, R. Xu, L. Philipson, *Proc. Natl. Acad. Sci. U.S.A.* **94**, 3352 (1997).
9. J. M. Bergelson *et al.*, *Science* **275**, 1320 (1997).
10. P. W. Roelvink *et al.*, *J. Virol.* **72**, 7909 (1998).
11. M. Bai, L. Campisi, P. Freimuth, *J. Virol.* **68**, 5925 (1994).
12. H.-Y. Yeh, N. Pieniazek, D. Pieniazek, H. Gelderblom, R. B. Luftig, *Virus Res.* **33**, 179 (1994).
13. Fiber gene sequences were obtained from the GenBank/EMBL databases. The accession numbers are P03275 (F2), L19194 (F4), M18369 (F5), X74660 (F8), X74659 (F9), X73487 (F12), X74658 and X74659 (F15), X14241 (F17), X94485 (F19), Y14242 (F28), X76548 (F31), X94484 (F37), P18047 (F40 long), and P14267 (F41 long). The figures were generated with RASMOL (Glaxo R&D, UK) and the F5K structure coordinates (Entrez MMDB Id 1398, Protein Data Bank accession number 1KNB).
14. D. Xia, L. Henry, R. D. Gerard, J. Deisenhofer, *Curr. Top. Microbiol. Immunol.* **199**, 39 (1995).
15. ———, *Structure* **2**, 1259 (1994).
16. Site-directed mutagenesis was performed with the Quikchange kit (Stratagene) and the baculovirus constructs pAcSG2-F5KN, pAcSG2-F9K, and pAcSG2-F41LK (*6, 10*). All DNA manipulations and protein expression and purification were as described (*6, 10*).
17. Fiber mutants were expressed in insect cells. Soluble and insoluble fractions were analyzed by protein immunoblotting and detection with a polyclonal antibody to F5K (*4*). Assessment of solubility was made by comparing the signal in the soluble and insoluble fractions with those of wild-type F5K expression in insect cells. The F5K-specific mAbs 3D9, 3F10, and 2C9 were generated for these studies by R. Wagner (ProtoProbe Inc., Milwaukee, WI). These mAbs recognize trimeric, but not heat-denatured fiber.
18. A549 cells (~10^5 per well) were preincubated with the competitor protein at increasing concentrations for 1 hour at 37°C. Ad.CMV-βgal (*9*) was added at a multiplicity of infection of 10 and incubated for 1 hour. Cells were washed twice with Dulbecco's modified Eagle's medium (DMEM) plus 5% fetal calf serum (FCS) and incubated overnight. Galactosidase activity was determined with the Galacto Light assay kit (Tropix Inc.).
19. Abbreviations for the amino acid residues are as follows: A, Ala; C, Cys; D, Asp; E, Glu; F, Phe; G, Gly; H, His; I, Ile; K, Lys; L, Leu; M, Met; N, Asn; P, Pro; Q, Gln; R, Arg; S, Ser; T, Thr; V, Val; W, Trp; and Y, Tyr.
20. P. W. Roelvink and T. J. Wickham, unpublished data.
21. I. Wilson *et al.*, *Cell* **37**, 767 (1984).
22. D. Brough *et al.*, *J. Virol.* **70**, 6497 (1996).
23. D. Einfeld *et al.*, *J. Virol.* **73**, 9130 (1999).
24. P. Freimuth *et al.*, *J. Virol.* **73**, 1392 (1999).
25. C. D. Rizzuto *et al.*, *Science* **280**, 1949 (1998).
26. P. D. Kwong *et al.*, *Nature* **393**, 648 (1998).
27. R. Wyatt *et al.*, *Nature* **393**, 705 (1998).
28. N. K. Sauter *et al.*, *Biochemistry* **31**, 9609 (1992).
29. W. Weis *et al.*, *Nature* **333**, 426 (1988).
30. M. Bewley, K. Springer, Y.-B. Zhang, P. Freimuth, J. M. Flanagan, *Science* **286**, 1579 (1999).

31. We thank all contributing scientists and technicians.

4 June 1999; accepted 23 September 1999

Genome Sequence of the Radioresistant Bacterium *Deinococcus radiodurans* R1

Owen White,[1] Jonathan A. Eisen,[1] John F. Heidelberg,[1] Erin K. Hickey,[1] Jeremy D. Peterson,[1] Robert J. Dodson,[1] Daniel H. Haft,[1] Michelle L. Gwinn,[1] William C. Nelson,[1] Delwood L. Richardson,[1] Kelly S. Moffat,[1] Haiying Qin,[1] Lingxia Jiang,[1] Wanda Pamphile,[1] Marie Crosby,[1] Mian Shen,[1] Jessica J. Vamathevan,[1] Peter Lam,[1] Lisa McDonald,[1] Terry Utterback,[1] Celeste Zalewski,[1] Kira S. Makarova,[2] L. Aravind,[2] Michael J. Daly,[3] Kenneth W. Minton,[3] Robert D. Fleischmann,[1] Karen A. Ketchum,[1] Karen E. Nelson,[1] Steven Salzberg,[1] Hamilton O. Smith,[1]* J. Craig Venter,[1]* Claire M. Fraser,[1]†

The complete genome sequence of the radiation-resistant bacterium *Deinococcus radiodurans* R1 is composed of two chromosomes (2,648,638 and 412,348 base pairs), a megaplasmid (177,466 base pairs), and a small plasmid (45,704 base pairs), yielding a total genome of 3,284,156 base pairs. Multiple components distributed on the chromosomes and megaplasmid that contribute to the ability of *D. radiodurans* to survive under conditions of starvation, oxidative stress, and high amounts of DNA damage were identified. *Deinococcus radiodurans* represents an organism in which all systems for DNA repair, DNA damage export, desiccation and starvation recovery, and genetic redundancy are present in one cell.

Deinococcus radiodurans is a Gram-positive, red-pigmented, nonmotile bacterium that was originally identified as a contaminant of irradiated canned meat (*1*). It has been isolated worldwide from locations rich in organic nutrients, including soil, animal feces, and processed meats, as well as from dry, nutrient-poor environments, including weathered granite in a dry Antarctic valley, room dust, and irradiated medical instruments (*2*). All species in the genus *Deinococcus*, in particular *D. radiodurans*, are extremely resistant to a number of agents and conditions that damage DNA, including ionizing and ultraviolet (UV) radiation and hydrogen peroxide (*3*). *Deinococcus radiodurans* is the most radiation-resistant organism described to

[1]The Institute for Genomic Research, 9712 Medical Center Drive, Rockville, MD 20850, USA. [2]National Center for Biotechnology Information, National Library of Medicine, Bethesda, MD 20894, USA. [3]Department of Pathology, Uniformed Services University of the Health Sciences, Bethesda, MD 20814, USA.

*Present address: Celera Genomics, 45 West Gude Drive, Rockville, MD 20850, USA.

†To whom correspondence should be addressed. E-mail: drdb@tigr.org

References and Notes

[8] **HCAR and MCAR: The Human and Mouse Cellular Receptors for Subgroup C Adenoviruses and Group B Coxsackieviruses**

Richard P. Tomko; Ruliang Xu; Lennart Philipson

Proceedings of the National Academy of Sciences of the United States of America, Vol. 94, No. 7. (Apr. 1, 1997), pp. 3352-3356.

Stable URL:

http://links.jstor.org/sici?sici=0027-8424%2819970401%2994%3A7%3C3352%3AHAMTHA%3E2.0.CO%3B2-P

[9] **Isolation of a Common Receptor for Coxsackie B Viruses and Adenoviruses 2 and 5**

Jeffrey M. Bergelson; Jennifer A. Cunningham; Gustavo Droguett; Evelyn A. Kurt-Jones; Anita Krithivas; Jeong S. Hong; Marshall S. Horwitz; Richard L. Crowell; Robert W. Finberg

Science, New Series, Vol. 275, No. 5304. (Feb. 28, 1997), pp. 1320-1323.

Stable URL:

http://links.jstor.org/sici?sici=0036-8075%2819970228%293%3A275%3A5304%3C1320%3AIOACRF%3E2.0.CO%3B2-I

[25] **A Conserved HIV gp 120 Glycoprotein Structure Involved in Chemokine Receptor Binding**

Carlo D. Rizzuto; Richard Wyatt; Nivia Hernández-Ramos; Ying Sun; Peter D. Kwong; Wayne A. Hendrickson; Joseph Sodroski

Science, New Series, Vol. 280, No. 5371. (Jun. 19, 1998), pp. 1949-1953.

Stable URL:

http://links.jstor.org/sici?sici=0036-8075%2819980619%293%3A280%3A5371%3C1949%3AACHG1G%3E2.0.CO%3B2-9

LINKED CITATIONS

[30] **Structural Analysis of the Mechanism of Adenovirus Binding to Its Human Cellular Receptor, CAR**

Maria C. Bewley; Karen Springer; Yian-Biao Zhang; Paul Freimuth; John M. Flanagan

Science, New Series, Vol. 286, No. 5444. (Nov. 19, 1999), pp. 1579-1583.

Stable URL:

http://links.jstor.org/sici?sici=0036-8075%2819991119%293%3A286%3A5444%3C1579%3ASAOTMO%3E2.0.CO%3B2-Z